Cell, Vol. 102, 657–670, September 1, 2000, Copyright ©2000 by Cell Press

# The Polar T1 Interface Is Linked to Conformational Changes that Open the Voltage-Gated Potassium Channel

**Daniel L. Minor, Jr.,*‡ Yu-Fung Lin,* Bret C. Mobley,* Abigail Avelar,* Yuh Nung Jan,* Lily Y. Jan,* and James M. Berger†**
*Howard Hughes Medical Institute and Departments of Physiology and Biochemistry
University of California, San Francisco
San Francisco, California 94143
†Department of Molecular and Cell Biology
University of California, Berkeley
Berkeley, California 94720

## Summary

**Kv voltage-gated potassium channels share a cytoplasmic assembly domain, T1. Recent mutagenesis of two T1 C–terminal loop residues implicates T1 in channel gating. However, structural alterations of these mutants leave open the question concerning direct involvement of T1 in gating. We find in mammalian Kv1.2 that gating depends critically on residues at complementary T1 surfaces in an unusually polar interface. An isosteric mutation in this interface causes surprisingly little structural alteration while stabilizing the closed channel and increasing the stability of T1 tetramers. Replacing T1 with a tetrameric coiled-coil destabilizes the closed channel. Together, these data suggest that structural changes involving the buried polar T1 surfaces play a key role in the conformational changes leading to channel opening.**

## Introduction

Voltage-gated cation channels act as molecular switches that control the generation of electrical signals by regulating ion flux across the cell membrane in response to membrane potential changes (Hille, 1992). Much of our understanding of how these proteins work comes from studies of voltage-gated potassium channels. These channels are denoted Kvx.y, where "x" represents the subfamily type and "y" represents a particular member of the subfamily (Chandy and Gutman, 1995). The first four subfamilies correspond to *Drosophila* channels *Shaker*, *Shab*, *Shaw*, and *Shal*, respectively.

Kv channels are tetramers in which each subunit contains six transmembrane segments, S1–S6 (Jan and Jan, 1997) (Figure 1A). The primary voltage sensor, S4, contains positively charged residues and responds to membrane depolarization with an outward movement that triggers the conformational change leading to channel opening (Sigworth, 1993; Mannuzzu et al., 1996; Cha and Bezanilla, 1997; Yellen, 1998). Kv channels also contain a highly conserved region responsible for potassium selectivity, the 'P loop' (Heginbotham et al., 1992). Aside from the P loop and S4, the most conserved domain in Kv channels comprises ~120 amino acids within the N-terminal cytoplasmic domain. This domain, called T1, plays a role in subunit tetramerization and subfamily-specific channel assembly (Li et al., 1992; Shen et al., 1993; Bixby et al., 1999).

We examined the mammalian brain and heart channel Kv1.2 by a combination of crystallographic analysis, protein stability studies, and electrophysiological characterization of structure-based channel mutations. Our results indicate that T1 has a direct role in channel gating. Mutations in the polar T1 subunit interface define distinct "hot spots" (Clackson and Wells, 1995) of residues that affect channel properties. These residues fall on complementary surfaces that form a highly conserved, unusually polar interface between T1 monomers, highlighting a potential general role for buried polar surfaces in protein complexes. Surprisingly, an isosteric mutation, T46V, in the T1 subunit interface stabilizes the closed channel and increases the stability of T1 tetramers, yet shows no significant perturbation to the T1 structure. Moreover, replacement of T1 with a four-stranded coiled-coil (Harbury et al., 1993) results in channels that open at much more hyperpolarized voltages. Together, these observations strongly suggest that T1 plays a role not only in channel assembly, but also in channel gating, and that conformational changes across the buried polar interface between subunits are a crucial part of the gating process.

## Results

### Structure of the Kv1.2 T1 Domain

The crystal structures of two versions of the T1 assembly domain of mammalian Kv1.2 (residues 33–125, denoted CORE, and 33–138, denoted +13C) were solved by molecular replacement to resolutions of 2.1 Å and 1.6 Å respectively, using a polyserine model derived from the T1 domain of *Aplysia* Kv1.1 (AKv1.1, residues 66–158) (Kreusch et al., 1998) (Figures 1B–1D and Table 1). The structures of the Kv1.2 T1 domain are similar to the structure of AKv1.1 ($C_\alpha$ atom rmsd's for superposition of CORE and +13C monomers onto the AKv1.1 monomer are 0.26 Å and 0.43 Å, respectively). CORE monomers appear to be folded into two domains (Figure 1C); an N-terminal domain composed largely of β sheet (residues 33–80) and a C-terminal domain that is largely α helical (residues 81–119). T1 has also been described in terms of "layers" (Kreusch et al., 1998), where layer 1 comprises the N-terminal domain and layers 2 and 3 comprise the C-terminal domain. +13C is identical to CORE ($C_\alpha$ atom rmsd's of 0.37 Å for residues 33–119) and includes an extra helix (residues 120–131) that is packed onto the C-terminal domain, also called layer 4 (Bixby et al., 1999). This helix was not in the polyserine model used for the solution. Its density became apparent during rebuilding and refinement. It has substantially higher B factors than the rest of the structure (average B factors for the $C_\alpha$ carbons of 33–119 and 120–131 are 23.3 and 47.8 $Å^2$, respectively), similar to differences seen between the C-terminal helix and the body of T1 in AKv1.1 and AKv3.1.

‡To whom correspondence should be addressed (e-mail: minor@itsa.ucsf.edu).

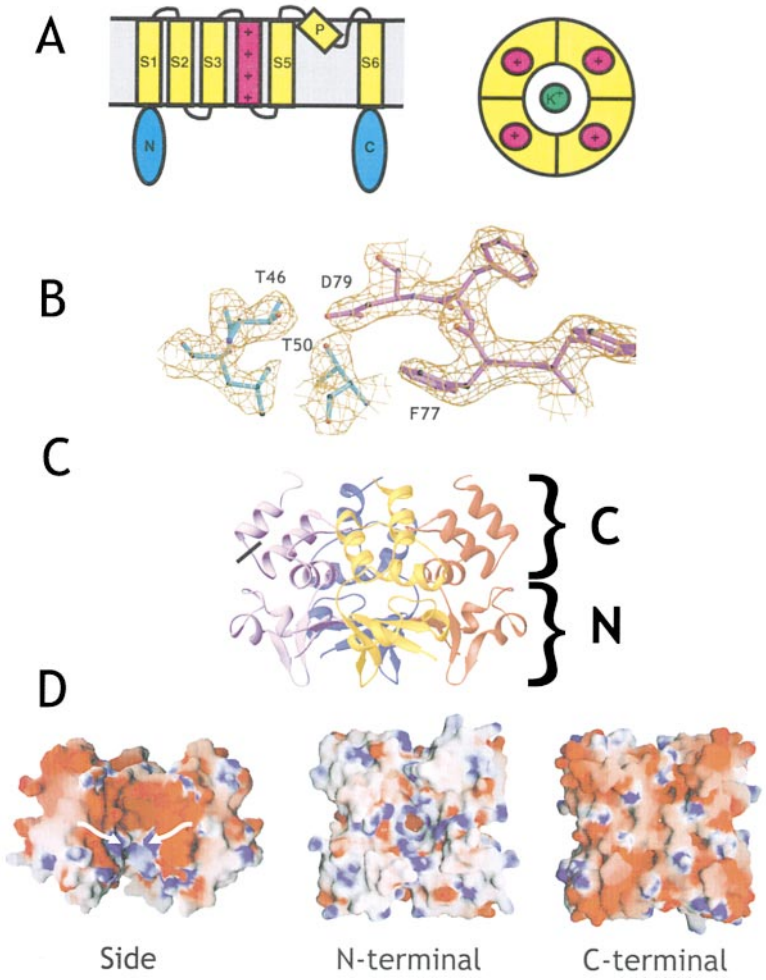


Figure 1. Structure of the Kv 1.2 T1 Domain

(A) Schematics of Kv channel structure. The left-hand cartoon represents a single subunit. S1–S3, S5, S6, and P (colored yellow) indicate the transmembrane segments and the selectivity filter, respectively. The S4 segment is labeled with "+" signs. The cytoplasmic domains are colored blue. The right-hand cartoon represents an extracellular view of a tetrameric channel. The green sphere represents a potassium ion.

(B) Electron density of the CORE interface containing T46 and D79 contoured at 1.3 $\sigma$, following averaging and density modification using $F_{obs}$ and model phases from the rigid-body refined, polyserine molecular replacement solution. Stick representation of the final refined model is shown with different subunits colored blue and magenta.

(C) Sideview RIBBONS (Carson, 1991) depiction of the Kv1.2 T1 +13C tetramer. Brackets indicate the N- and C-terminal domains of a single subunit. The black bar indicates the end of the CORE structure; the extra C-terminal helix in +13C follows.

(D) Molecular surface and electrostatic potentials ($\pm$7 $k_bT/e$) for +13C T1 calculated with GRASP (Nichols et al., 1991). Views are (left to right): cutaway view from the side with one subunit deleted to reveal the central cavity and polar subunit interfaces. White arrows indicate the narrowest constriction in the central cavity. The molecule is oriented as in (C). Views from the N-terminal side and from the C-terminal side.

Kv1.2 T1 monomers of both CORE and +13C assemble into tetramers. The 4-fold axis of the molecule runs through an hourglass shaped cavity filled with crystallographically visible water molecules. The cavity opens at the N-terminal side of the protein, narrows to a diameter of ~7 Å between the N- and C-terminal domains, expands into a small chamber that is ~14 Å at its widest, ~9 Å long, and is occluded at its C-terminal end (Figure 1D).

As with the AKv1.1 T1 structure, the most striking feature of the Kv1.2 T1 tetramer is that the subunit interfaces are extremely polar. Of the thirty sidechains that make contacts across the interface, twenty-one are polar (Table 2). Buried polar interactions tend to be destabilizing in proteins (Hendsch and Tidor, 1994; Waldberger et al., 1995; Wimley et al., 1996) and such a large, buried polar interface is extremely unusual. Indeed, most assembly domain interfaces in constitutively-associated

Table 1. Molecular Replacement and Refinement Statistics

| Data collection and refinement | Core | +13C | VCORE |
|---|---|---|---|
| Wavelength (Å) | 1.54 | 0.961 | 1.000 |
| Resolution (Å) | 20–2.1 | 20–1.6 | 30–1.6 |
| $R_{sym}$* (Last shell) (%) | 7.6 (28.3) | 3.0 (16.6) | 4.8 (37.1) |
| Completeness (%) | 94.5 | 86.4 | 96.1 |
| Space group | $P2_12_12_1$ | $P2_12_12_1$ | $P2_12_12_1$ |
| Cell dimensions (Å) (a,b,c) | 76.26, 78.24, 125.32 | 51.77, 82.03, 96.28 | 76.39, 78.40, 126.92 |
| Number of reflections | 42,293 | 49,725 | 97,159 |
| Number of monomers/a.u. | 8 | 4 | 8 |
| $R_{work}$ ($R_{free}$**) (%) | 22.6 (26.5) | 23.8 (27.8) | 23.4 (27.9) |
| No. atoms: protein/water | 5944/574 | 3411/238 | 5944/590 |
| rmsd bond lengths/angles (Å/deg) | 0.006/1.13 | 0.008/1.40 | 0.008/1.40 |

* $R_{sym} = \Sigma\Sigma_j|I_j - \langle I\rangle|\Sigma I_j$, where $I_j$ is the intensity measurement of reflection j and $\langle I\rangle$ is the mean intensity for multiply recorded reflections.
** $R_{work,free} = \Sigma||F_{obs}| - |F_{calc}||/|F_{obs}|$, where the working and free R factors are calculated using the working and free reflection sets, respectively. The free reflections (10% of the total) were held aside throughout the refinement.

Table 2. Kv1.2 T1 Subunit–Subunit Contact Residues

| Side A residue | Side B residue | Distance Å | Side A residue | Side B residue | Distance Å |
|---|---|---|---|---|---|
| R34 NH2 | N38 Oδ1 | 3.50 | T50 Oγ1 | D79 Oδ2 | 2.65 |
| R34 NH1 | D70 Oδ2 | 3.22 | D86 Oδ1 | R82 Nϵ | 2.73 |
| R34 NH2 | R73 Nϵ | 3.69 | Y90 Cδ1 | N81 Nδ2 | 3.52 |
| R34 NH2 | E75 Oϵ2 | 3.40 | Y90 OH | I108 Cγ1 | 3.46 |
| R34 NH2 | F77 Cδ1 | 3.65 | Y90 OH | E111 Oϵ1 | 3.94 |
| L42 Cδ2 | R82 NH1 | 3.95 | Q93 Nϵ2 | S40 Oγ | 2.84 |
| R43 O | G41 Cα | 3.55 | Q93 Nϵ2 | D79 Oδ1 | 2.85 |
| F44 Cα | S40 O | 3.42 | Q93 Nϵ2 | R80 N | 3.54 |
| F44 Cϵ2 | R82 Nϵ | 3.32 | R97 Nϵ | D107 Oδ2 | 3.67 |
| E45 Oϵ1 | N38 Oδ1 | 3.29 | R97 NH1 | I108 Cγ1 | 3.91 |
| E45 N | S40 O | 2.98 | R97 NH2 | E111 Oϵ2 | 2.37 |
| E45 Cγ | G41 Cα | 3.77 | R99 NH1 | P105 Cβ | 3.37 |
| E45 Oϵ2 | R43 NH1 | 3.06 | R99 NH2 | D107 Oδ2 | 2.74 |
| E45 O | F77 Cζ | 3.76 | V102 Cγ2 | N103 Cβ | 3.42 |
| T46 Oγ1 | D79 Oδ1 | 2.70 | | | |
| T46 Oγ1 | D79 Oδ2 | 3.75 | | | |
| Q47 Nϵ2 | D79 Oδ2 | 2.80 | | | |

All residues are within 4 Å of residues on the opposite side of the interface. A slightly larger cutoff of 4.5 Å identifies one other residue, L89, which was also included in the alanine scan.

multimeric protein complexes are composed of nonpolar, well-packed residues (Janin et al., 1988; Jones and Thornton, 1997). The polar nature of the residues in the T1 interface is strongly conserved (Kreusch et al., 1998), suggesting that the stability penalties incurred by these types of interactions are balanced against a strong functional requirement.

In contrast to the subunit interfaces, the outer surface of the T1 tetramer is relatively hydrophobic. From a topological consideration of the intact channel (see below), it seems likely that this surface of T1 contacts other parts of the channel, such as the C-terminal cytoplasmic domains and the cytoplasmic loops of the transmembrane domain.

### Disruption of a Buried Polar Interaction Affects Channel Gating

Our attention was drawn to a specific buried, polar interaction at the subunit interface. T46 has been implicated as a site for protein kinase A regulation of Kv1.2 (Huang et al., 1994). The γ-hydroxyl group of this residue is completely buried from solvent and participates in a bidentate hydrogen bond with the sidechain carboxylate oxygens of D79. T46 and D79 are part of a large, buried hydrogen-bonding network in which T50, Q47, and Q93 also interact with D79 (Figure 2A). To eliminate the T46-D79 interaction, we made the isosteric change T46V, thereby replacing the hydrogen bonding group with a methyl group while conserving the sidechain volume. Surprisingly, the T46V channel was more difficult to open than the wild-type channel when expressed in *Xenopus* oocytes (a shift of +24.3 mV in the midpoint activation voltage, $V_{1/2}$). This mutant also opened more slowly (Figure 2B).

T1 domains bearing T46V form tetramers resembling wild type in size by gel filtration and analytical equilibrium centrifugation (data not shown). Strikingly, the T46V mutant is more stable than the wild-type T1 domain (Figures 2C and 2D), as measured by denaturant unfolding (Pace et al., 1989) using circular dichroism (CD).

Under conditions where both folded and unfolded forms of the protein are present, the T1 CD signal was concentration dependent (Figure 2E). There was no change in the CD signal of T1 over a similar protein concentration range under native conditions (Figure 2E). Further evidence for coupling between folding and assembly was obtained by examining a +13C mutant that introduces a charge in the interface, T46D. CD experiments show little evidence for folded structure in T46D under conditions where the wild-type T1 is folded and tetrameric (Figure 2F). Gel filtration chromatography indicates that the T46D mutation disrupts the tetrameric state of T1 (Figure 2F, inset). The precise oligomerization state of T46D is not clear since its migration on the gel filtration column did not cleanly match the expected size for either a monomer or a dimer. Nevertheless, these data show that this mutation disrupts the native, tetrameric state of T1, accounting for the failure of T46D mutants to form functional channels. Taken together, these results demonstrate that folding and assembly of T1 are linked, the global stability of the T1 tetramers can be altered by mutations that directly affect the subunit interface, and that these mutations can have effects on the assembly of the T1 tetramer.

### Structure of the T46V T1 Mutant

In order to investigate the structural consequences of T46V mutation, we solved the crystal structure of CORE containing the T46V mutation (VCORE) to a resolution of 1.6 Å (Table 1). No gross rearrangements of the tetramer result from the mutation (Figure 3A). The rmsd for superposition of the corresponding $C_\alpha$ backbone atoms of +13C and VCORE tetramers is ~1Å (rmsd's = 0.76 Å for $C_\alpha$ atoms), similar to the differences between our structures and the differences between these structures and other published T1 domains. The structural changes caused by the mutation were restricted to the area near the change. V46 is shifted ~1 Å away from the position of T46, increasing the distance between the γ-methyl of the sidechain (hydroxyl in the wild type) and the D79 carboxylate oxygens by 0.3 and 1.3 Å, respectively (Fig-

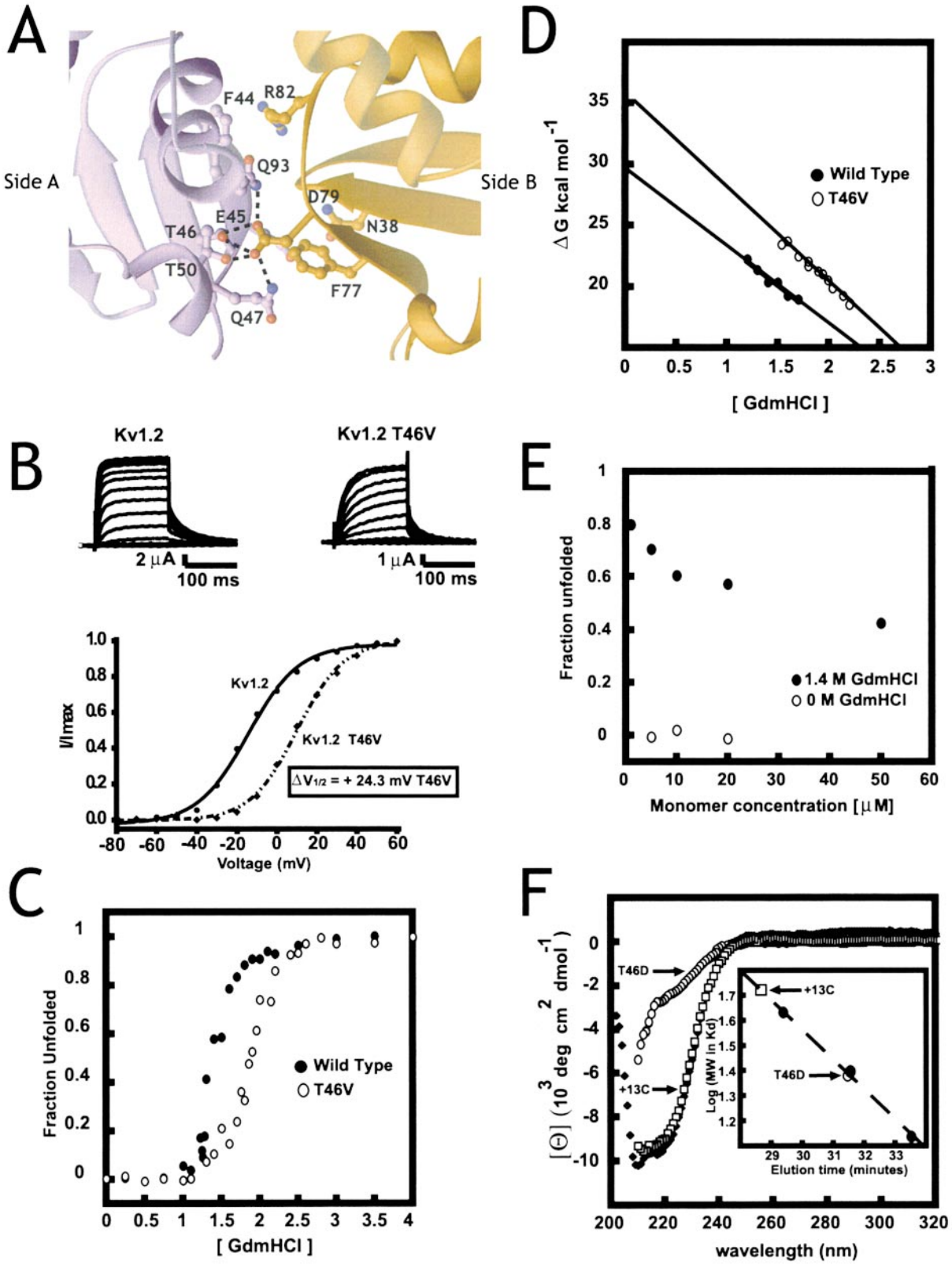
A
Side A
Side B
F44
R82
Q93
D79
E45
N38
T46
T50
F77
Q47
B
Kv1.2
Kv1.2 T46V
2 μA
100 ms
1 μA
100 ms
I/Imax
Kv1.2
Kv1.2 T46V
ΔV1/2 = + 24.3 mV T46V
Voltage (mV)
C
Fraction Unfolded
Wild Type
T46V
[ GdmHCl ]
D
ΔG kcal mol-1
Wild Type
T46V
[ GdmHCl ]
E
Fraction unfolded
1.4 M GdmHCl
0 M GdmHCl
Monomer concentration [μM]
F
[Θ] (10^3 deg cm^2 dmol^-1)
T46D
+13C
Log (MW in Kd)
Elution time (minutes)
wavelength (nm)

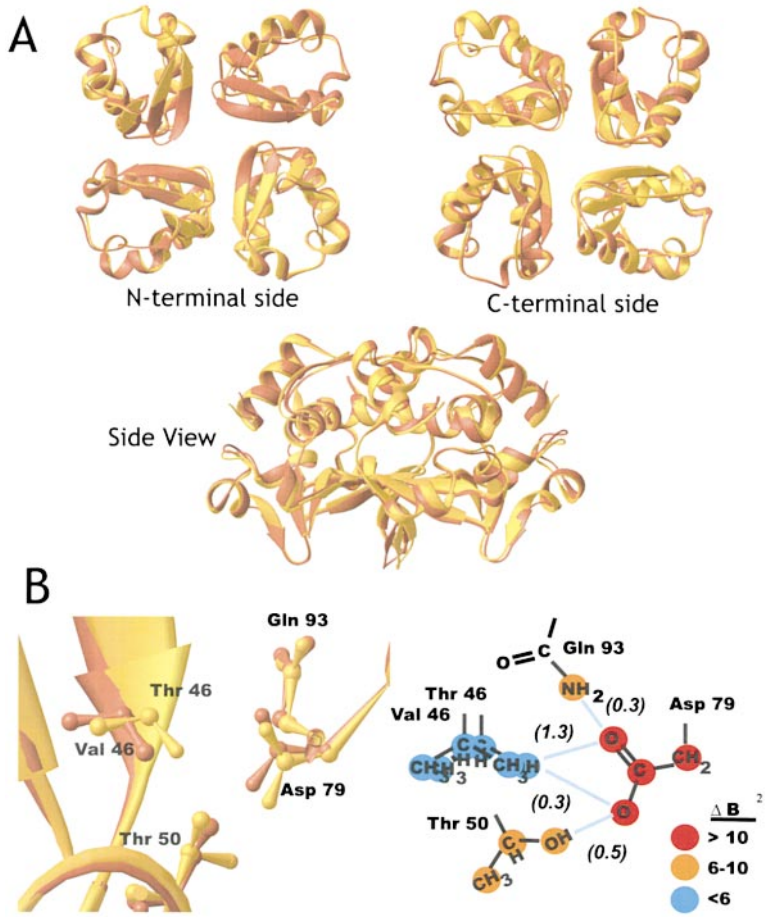


Figure 3. Structural Comparison of Wild-type and T46V (VCORE) T1 Domains

(A) RIBBONS (Carson, 1991) depiction of the superpositions for residues 33–119 of wild-type T1 (yellow) and VCORE (red) based on a comparison of $C_\alpha$ atoms.

(B) View of local structural rearrangements caused by the T46V mutation. The right-hand side shows a schematic of the interactions. Distance changes are indicated by the gray lines. The change in Å is shown in parenthesis. Changes in B factors are also shown.

ure 3B). T50 also moves away from D79 by 0.5 Å. Nonetheless, D79 remains within hydrogen bonding distance of T50, Q47, and Q93.

Since the global features of the T1 domain are unchanged by the mutation, it seems unlikely that the rest of the channel would be able to "sense", through contact with the exterior surface of T1, whether it was connected to wild-type or mutant T1 domain. Thus, together with the functional studies, the crystallographic analysis suggests a mechanistic explanation for the functional effects of the T46V mutation; namely, this mutation alters voltage gating by affecting the energetics of a conformational change in the T1 subunit interface that is coupled to channel opening.

Figure 2. Mutations in the T1 Subunit Interface Affect Channel Activity and T1 Stability

(A) The subunit interface and hydrogen bonding network around T46. "Side A" is colored purple and "side B" is colored orange. Dashed lines indicate hydrogen bonds.

(B) Two electrode voltage clamp recordings from *Xenopus* oocytes expressing wild-type or T46V Kv1.2 channels. The normalized conductances (I/Imax), obtained from tail current and $\Delta V_{1/2}$ (error $\pm$ 2 mV) are shown.

(C) Measurement of the thermodynamic stability of T1 tetramers. Fraction unfolded protein as a function of guanidinium hydrochloride [GdmHCl] measured by circular dichroism. Filled circles indicate wild type, open circles indicate T46V.

(D) Plot of the free energy of folding ($\Delta G$) vs. denaturant for the unfolding curves shown in (C). $\Delta\Delta G$ is for T46V in 0 M GdmHCl at 1 M standard state is 5.7 kcal mol$^{-1}$, defined as $\Delta G_{mutant} - \Delta G_{wild\text{-}type}$. The intercept ($\Delta G_{0M\ GdmHCl}$), slope (Pace et al., 1989), and correlation coefficient, $R^2$, for the linear fit of the data are: wild type, 29.9 kcal mol$^{-1}$, 6.54 kcal mol$^{-1}$ mol$^{-1}$, 0.98; T46V, 35.6 kcal mol$^{-1}$, 7.36 kcal mol$^{-1}$ mol$^{-1}$, 0.96.

(E) Folding of T1 is concentration dependent. Fraction unfolded +13C is shown as a function of monomer concentration at 0 M GdmHCl and 1.4 M GdmHCl.

(F) Introduction of a charge in the T1 subunit interface results in unstructured, nontetrameric T1 domains. Circular dichroism spectra at 20°C are shown for: 10 $\mu$M +13C under native conditions (filled diamonds) and in the presence of 1 M GdmHCl (open squares) and 20 $\mu$M T46D in the presence of 1 M GdmHCl (open circles). Inset: Gel filtration data (Pharmacia Superdex 200, 100 mM KCl, 1M GdmHCl, 1 mM EDTA, and 20 mM HEPES [pH 7.5]). Black circles indicate ovalbumin (43.0 kDa), chymotrypsinogen (25.0 kDa), and RNaseA (13.7 kDa). The standard curve [Log (molecular weight in kDa) vs. elution time] is shown (slope 5.16 and intercept −0.12). The open square and open oval indicate +13C and T46D. Molecular weights for these proteins are 52.2 kDa for +13C (expected tetramer size, 52.1 kDa) and 24.1 kDa for T46D (expected monomer and dimer, 13.0 and 26.0 kDa). T46D required the presence of denaturant to be soluble and was not significantly soluble in conditions of lower denaturant.

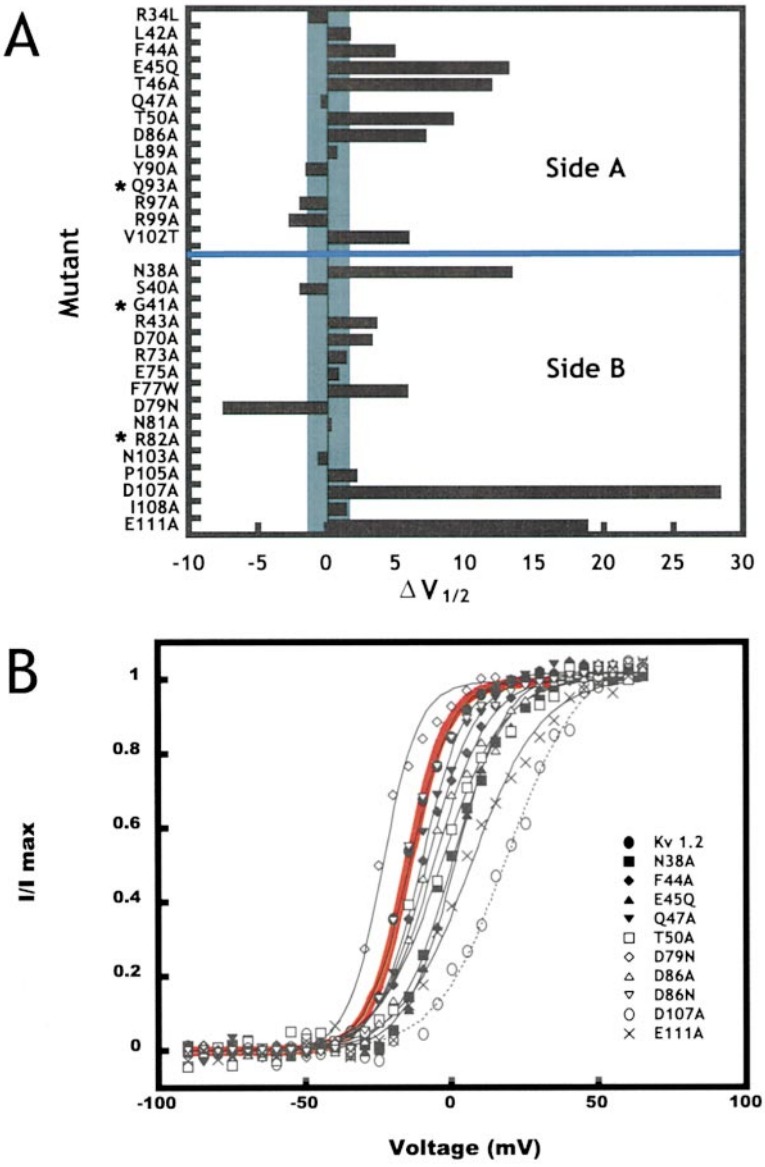


Figure 4. Alanine Scanning Identifies T1 Interface Positions That Have Effects on Gating

(A) $\Delta V_{1/2}$ for Kv1.2 T1 interface mutants measured from tail currents at −80 mV. Values are relative to wild-type Kv1.2. Gray stripe indicates the limits of certainty (± 2 mV). Asterisk (*) denotes positions for which no functional mutants were observed.

(B) Plots of normalized conductance (I/Imax), as a function of voltage obtained from tail current measurements.

### Scanning Mutagenesis of the T1 Subunit–Subunit Interface

To characterize the energetic importance of all of the residues in the T1 subunit interface with respect to channel gating, we examined the interface by scanning mutagenesis (Wells, 1991). Residues that make contacts across the subunit interface were identified from analysis of the +13C structure and defined as those having sidechain atoms ≤ 4 Å away from atoms on the other side of the interface ("side A" contains T46 and "side B" contains D79) (Table 2).

Only a subset of the sidechain truncations had significant effects (Figures 4A and 4B). Seven of the thirty alanine substitutions in the interface affected voltage gating ($\Delta V_{1/2} \geq |5$ mV|). These changes occupy positions on both sides of the interface (side A: F44A, T46A, T50A, and D86A; side B: N38A, D107A, and E111A). Half of the alanine substitutions had no significant effect on channel gating (side A: L42A, R43A, Q47A, L89A, Y90A, and R99A; side B: S40A, D70A, R73A, E75A, N81A, R97A, N103A, and P105A). We were unable to observe functional channels for eight alanine mutants (R34A, G41A, E45A, F77A, D79A, R82A, Q93A, and V102A). To try to obtain data for these positions, we made other mutations that altered the nature of the atoms in the interface but that were conservative with respect to sidechain shape and volume. These mutations defined four more positions that affect the $V_{1/2}$ of the channel (E45Q, F77W, D79N, and V102T). R43 did not tolerate alanine but was unaffected by the change R43L. Three residues (G41, R82, and Q93) did not tolerate any of the substitutions that we tested.

The mutations in the T1 interface that affect channel gating form distinct surface patches, or "hot spots" (Clackson and Wells, 1995) on both sides of the subunit interface and at all altitudes of the N- and C-terminal domains (Figure 5A). The patches in the N-terminal portion of T1 form complementary surfaces that interact

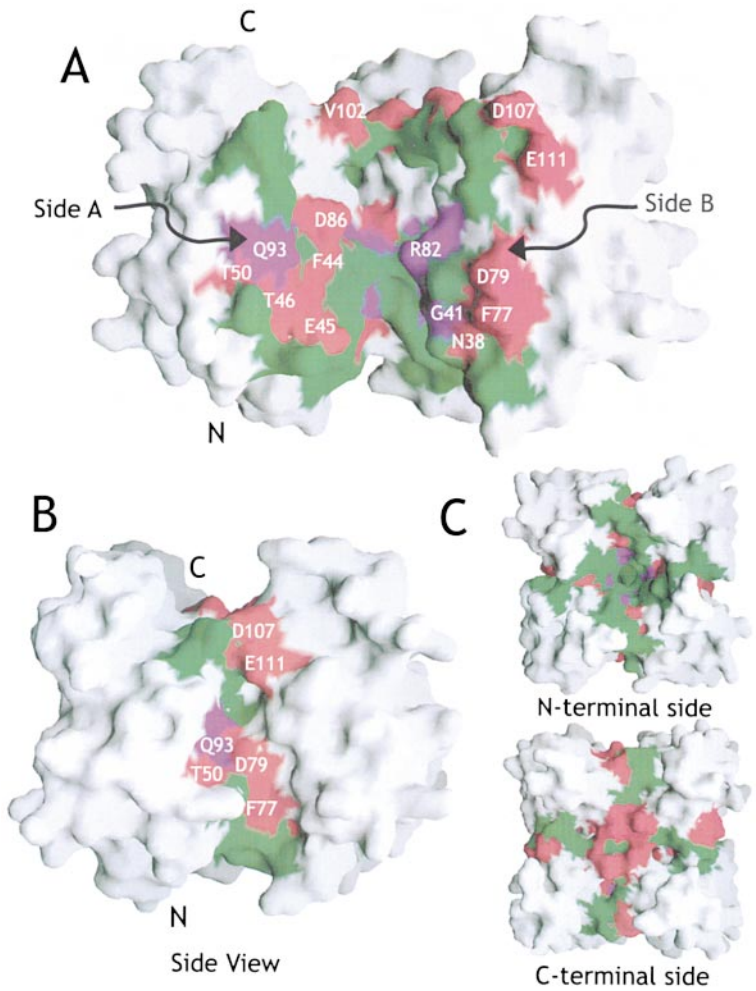


Figure 5. T1 Interface Mutations That Affect Gating Cluster into "Hot Spots" on the Interface Surface

(A) Molecular surface, cutaway view of the T1 tetramer seen from the side with one subunit deleted. "Side A" and "side B" of the interface are indicated. Residues are color-coded according to their effects on channel gating. Red indicates $\Delta V_{1/2}$ of $\geq |5$ mV|, green indicates no significant change, and purple indicates residues intolerant to change.

(B) and (C), external views of the T1 tetramer revealing the accessibility of hot spot residues from the exterior of T1.

across the subunit interface comprising three groups: members of the hydrogen bonding network around D79, the residues that were completely intolerant to change (G41, R82, and Q93), and residues F44 and D86 that interact with R82 to form the tightest constriction in the central cavity.

Some of the mutation-sensitive residues are arranged in a stripe that is accessible from the exterior of T1 (Figures 5B and 5C), including amino acids that form a groove between the T1 subunits (Figure 5B) and that are partially exposed on the C-terminal part of the protein (Figure 5C). These data raise the possibility that these partially accessible residues interact with other parts of the channel. In contrast, mutations of most of the residues accessible from the N-terminal side of T1 have little effect on gating.

It is striking that most of the mutations that have significant effects on $V_{1/2}$ shift the activation curves to more positive potentials. This behavior is consistent with the idea that buried polar interactions are destabilizing relative to replacement with nonpolar residues (Hendsch and Tidor, 1994; Waldberger et al., 1995; Wimley et al., 1996; Hendsch and Tidor, 1999) and stands in contrast to the generally destabilizing effects of alanine substitution seen in classical protein–protein interfaces in which the major contacts are nonpolar (Cunningham and Wells, 1989; Clackson and Wells, 1995). The absence of left-shifted mutants may reflect technical limitations since mutations that are deleterious to T1 folding prevent efficient channel assembly. Together with the strong conservation of residues in this interface (Kreusch et al., 1998), our scanning mutagenesis experiments suggest that T1 has not evolved to be a maximally stable complex; the T1 subunit interactions can be made stronger by replacement of the polar residues with nonpolar side-chains. Instead, it seems that T1 interactions have evolved so that the tetramer assembles but is poised for a facile conformational change.

### Replacement of T1 with a Different Tetramerization Domain Alters Channel Properties

Our mutagenesis experiments suggest that T1 plays a role in affecting the balance between the closed and open states of the channel. To test this hypothesis further, we deleted the T1 domain or replaced it with a structurally unrelated tetramerization domain, a four-stranded coiled-coil, p-LI (Harbury et al., 1993) (Figure 6A). To evaluate whether the coils imposed strain on a particular conformation of the channel, we connected p-LI to the membrane-spanning portion of the channel through the natural linker sequence present between the end of the T1

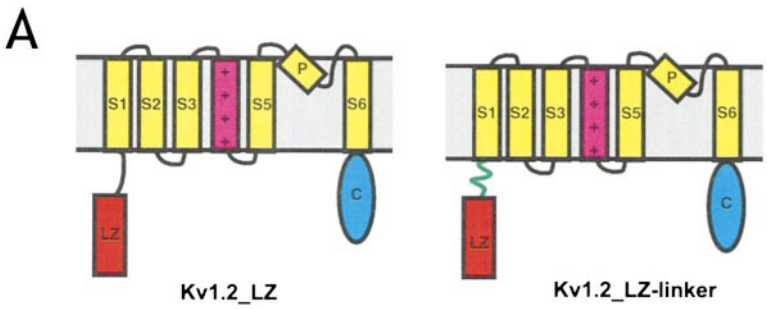


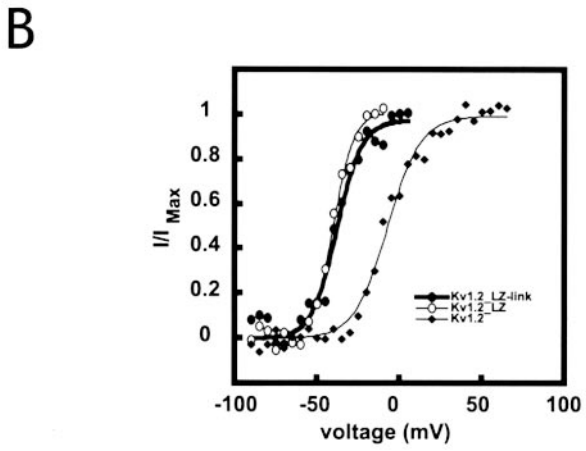


Figure 6. T1 Assembly but Not Gating Function Can Be Replaced with a Four-Stranded Coiled-Coil

(A) Schematic cartoon of the Kv1.2_LZ and Kv1.2_LZ-linker proteins in which the T1 domain was replaced with the four-stranded coiled-coil, p-LI (Harbury et al., 1993). The natural, and glycine-serine linkers (green wavy line) are depicted (see text).

(B) Plots of normalized conductance (I/Imax), obtained from tail current measurements recorded from *Xenopus* oocytes for Kv1.2_LZ and Kv1.2_LZ-linker are shown relative to wild-type. The $\Delta V_{1/2}$ of the mutants was −30.7 and −32.7 mV ± 2, respectively.

structure and S1 (30 residues) or through a thirteen residue glycine-serine linker.

No functional channels were detected in *Xenopus* oocytes expressing Kv1.2 in which T1 was deleted. This is probably due to failed channel assembly, since deletion of T1 from Kv-type channels dramatically influences the efficiency of channel formation (Zerangue et al., 2000). In contrast, replacement of the T1 domain by the coiled-coil assembly sequence yielded functional channels that were significantly easier to open. The $V_{1/2}$ was shifted in the hyperpolarized direction (approximately −30 mV) regardless of the linker used, suggesting that this shift reflects the absence of T1 on the relative stability of the open and closed states. Interestingly, these channels activated more slowly than wild type, similar to *Shaker* channels missing T1 (Kobertz and Miller, 1999; Zerangue et al., 2000). These data demonstrate that an artificial tetramerization domain can assume the assembly function, but not the gating function, of T1. Indeed, removal of T1 from Kv1.2 has profound effects on the stability of the closed state of the channel supporting the idea that T1 plays some role in the channel gating process.

## Discussion

Voltage-gated ion channels are molecular switches that respond to changes in the cell membrane potential (Hille, 1992). Over the past decade, mutational analysis coupled with chemical labeling methodologies has demonstrated that the transmembrane segments of voltage-gated potassium (Kv) channels undergo a conformational change as the protein switches between closed and open states (Sigworth, 1993; Yellen, 1998). With rare exceptions (Elkes et al., 1997; Johnstone et al., 1997; Cushman et al., 2000), most mutations characterized to date have been located in the transmembrane segments or their connecting loops (Sigworth, 1993; Yellen, 1998). Hence, the current working models of gating have focused on conformational changes in the transmembrane segments.

Kv channels share a common N-terminal cytoplasmic domain, T1, that promotes the formation of functional tetramers and prevents coassembly of Kv channel subunits from different families (Li et al., 1992; Shen et al., 1993). The structure of T1 from mammalian Kv1.2, *Aplysia* Kv1.1 (Kreusch et al., 1998; Bixby et al., 1999), and *Aplysia* Kv3.1 (Bixby et al., 1999) reveals a tetrameric protein with two very unusual features. First, the subunits are arranged around a central water-filled cavity that is coincident with the molecular 4-fold axis of symmetry. Second, the subunit interface consists primarily of a highly conserved, buried polar core of residues (Kreusch et al., 1998).

One general concern with mutations that change ion channel function is that the mutation may act by direct or indirect mechanisms (Ascher and Stevens, 1992). A vivid example of this complication occurs in a recent

mutagenesis and structural study of T1. Cushman et al. reported three mutations in the C-terminal apex of T1 that affect channel gating (Cushman et al., 2000) leading to the suggestion that this region of T1 is tightly coupled to the channel's gating states. Unfortunately, all three mutations alter the surface of the mutant T1 structures, rendering it impossible to determine whether T1 itself, or a propagated change from the mutant T1 to critical parts of the gating machinery outside of T1, affects channel gating.

Here, we report data that suggest an active role for T1 in the gating process. Our observations indicate that the conformational changes leading to channel opening are not limited to the transmembrane segments but also include changes at the buried polar interfaces between the highly conserved cytoplasmic domains of Kv subunits. Isosteric replacement of a residue (T46V) involved in a buried hydrogen bond network in this interface increases the stability of the closed state of the channel relative to the open state, as well as the stability of T1 itself, while causing only a minimal, local change in the structure. While the conformation of the isolated T1 is likely to be a good model of T1 in the closed channel, the exact structural and energetic contexts of T1 in the open channel are probably very different from those of T1 in denaturant. Nevertheless, given that a mutation at the T1 interface can stabilize both the T1 tetramer and the closed state of the channel without significantly altering the T1 tetramer structure, the gating effect of this mutation implicates a structural rearrangement across the subunit interface during channel opening.

An examination of the interface residues by scanning mutagenesis experiments reveals sidechains on both sides and all altitudes of the structure that have effects on channel gating. Similar to other scanning mutagenesis studies (Clackson and Wells, 1995; Cabral et al., 1998; Pons et al., 1999), the energetically critical residues are clustered in "hot spots" that include the sidechains that are most sensitive to mutation and those that are intolerant to even conservative changes. Most of the hot spots occur on complementary opposing surfaces of the N-terminal portion of the interface between T1 monomers, fitting the general picture that energetically important residues in protein–protein interfaces form matching complementary surfaces (Clackson and Wells, 1995). This complementarity suggests that the conformational change experienced by T1 during channel opening involves portions of the T1 structure within the polar subunit interface and supports the relevance of the structure of the isolated T1 domain with respect to the structure of the intact channel.

Although good complementarity exists between the hot spots on each side of the T1 interface at the altitude of the N-terminal domain, an interesting exception occurs in the C-terminal domain. Mutations D107A and E111A cause large positive shifts in the $V_{1/2}$ of the channel. These residues form a contiguous accessible surface on side B of the C-terminal domain. The hot spot formed by D107 and E111 is unpaired in the T1 domain; mutation of the T1 partners of these residues (R97 and R99, and Y90 and R97, respectively) has minimal effect on channel properties. D107 and E111 together with other hot spot surfaces accessible from the outside of T1 (T50, D79, Q93, F77, and V102) (Figures 5B and 5C) form good candidates for points of contact with other parts of the channel that may provide a means for energetic coupling to T1.

Both positions probed in the Cushman et al. study make subunit–subunit contacts (Table 2) and were examined here (Kv1.2 V102 and N103 correspond to AKv1.1 V135 and N136), although V102 is not in the buried interface having 63% average sidechain accessible surface area. We find that an isosteric change, V102T, causes a shift of similar magnitude to a much more radical change in AKv1.1 (V135R), +6.0 mV vs. +7.0 mV, whereas truncation of the sidechain to alanine at V102 is not tolerated. V102 is therefore a possible point of interaction with other parts of the channel. With respect to the other position, Cushman et al. find that N136A shifts the activation curve (−4.0 mV) and changes the interior diameter of T1. In contrast, we find that N103A has no significant effect (−0.7 mV).

### Scanning Mutagenesis Points to a Global Conformational Change during Gating

What is the nature of the T1 conformational change during gating? It seems likely that some disruption or rearrangement of the T1 interface occurs during gating, otherwise, it is hard to explain the effect of a mutation like T46V. In the extreme, the conformational change may involve complete disengagement of the T1 domains from each other. Alternatively, the conformational change in T1 may involve a rotation of the domains relative to each other. As these changes occur, residues in the subunit interface may interact with other parts of the channel that become revealed. Since buried polar cores between protein domains have been suggested to facilitate domain mediated structural rearrangements (Hirsch et al., 1999), these hypothetical models provide teleological explanations for the curious character of the buried polar core between the subunits. It is important to note that, although our experiments clearly point to a structural change in T1 upon channel gating, they do not reveal the precise nature of the change.

### T1's Relation to the Rest of the Channel

Since the initial elucidation of the structure of a T1 domain (Kreusch et al., 1998), the question regarding the orientation of T1 with respect to the remainder of the channel has remained open (Yellen, 1998; Kobertz and Miller, 1999). Placing the C-terminal side toward the intracellular surface of the membrane near the likely position of the cytoplasmic loops between the transmembrane segments, yields an orientation that is consistent with the positions of the hot spots on the C-terminal face and lateral sides of T1 (an orientation also suggested by Cushman et al.). This orientation positions T1 directly below the ion-conducting pathway of the channel (Figure 7), such that the 4-fold axis of symmetry that runs through T1 is coincident with the channel pore, but presents an interesting problem in threading the polypeptide chain.

The C-terminal end of the T1 structure is aimed toward the molecular 4-fold axis and connects to S1 on the lipid-facing periphery of the transmembrane helical bundle (Monks et al., 1999) by the T1–S1 linker. This linker may

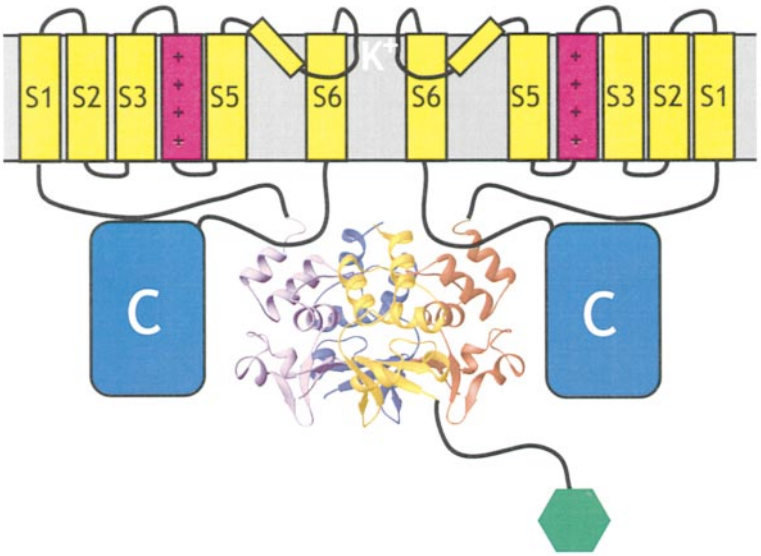


Figure 7. Cartoon of an Intact Kv Channel

The 4-fold axis in T1 is aligned with the 4-fold axis presumed to run through the channel pore. Transmembrane segments and C-terminal domains are indicated for two subunits and colored as in Figure 1. The green hexagon represents the N-terminal inactivation ball present in some Kv channels. Only one inactivation ball is shown for clarity.

play a role in communicating structural changes between T1 and the transmembrane parts of the channel, as domain swapping experiments indicate that changes in the amino acid composition of this linker influence channel gating properties (Chiara et al., 1999). The polypeptide chain exits the membrane following the last transmembrane segment, S6, thought to line the ion conduction pore (Lopez et al., 1994; Liu et al., 1997). Thus, the chain following S6 may need to thread outward past T1 into an area where there would be space for C-terminal cytoplasmic domains (~100–400 amino acids), to fold or exist as random coil structure. A disulfide bond can occur between a cysteine on the periphery of T1 immediately prior to the first amino acid in our structure and the cytoplasmic C-terminal domain (Schulteis et al., 1996), suggesting physical contact between these domains. Regardless of the location of the C-terminal cytoplasmic domains, the placement of T1 directly underneath the ion conduction pathway leaves major questions regarding how modulators such as the N-terminal inactivation ball or cytoplasmic blockers access their targets (Armstrong and Hille, 1972; Isacoff et al., 1991; Holmgren et al., 1997).

### What Exactly Is "The Gate"?

The demonstration that Kv channels can trap quaternary amines inside (Armstrong and Hille, 1972) provided the first evidence for a cytoplasmic activation gate. Since then, the exact molecular nature of the gate has remained unknown (Yellen, 1998). The putative position of T1 under the pore suggests that it could be part of a cytoplasmic gate, directly or indirectly controlling access to the ion conduction pore. In the KcsA structure, the positions that form the narrowest part of the pore occur at the bundle crossing of the M2 helices at the expected altitude where state-dependent reactivity changes occur in cysteine mutations of six consecutive residues of the *Shaker* S6 transmembrane segment (Doyle et al., 1998; Yellen, 1998), suggesting the existence of a "trap door" (Holmgren et al., 1997; Liu et al., 1997). While this comparison may indicate that the gate resides in the membrane, it is notable that the residues that make the helical bundle crossing in KcsA correspond to an extremely well-conserved amino acid sequence in S6 of Kv channels, Pro-Val-Pro, not present in KcsA. Mutations of either proline significantly change Kv channel gating properties (Elkes et al., 1997; Johnstone et al., 1997; Liu et al., 1997). Prolines in transmembrane helices commonly cause breaks or large kinks in the helical structure (von Heijne, 1991; Javadpour et al., 1999) questioning not only the structural correspondence in this part of the pore between KcsA M2 (which lacks prolines) and S6 of Kv channels (del Camino et al., 2000), but also the idea that this region is the gate for Kv channels. Since T1 appears to undergo a conformational change coupled to channel opening and is likely to reside under the cytoplasmic exit of the pore from the membrane, it is possible that T1, perhaps together with parts of the T1–S1 linker and portions of S6, contributes to the cytoplasmic gate.

The exact physical nature of the gate is imperfectly understood. Scanning mutagenesis experiments suggest that many parts of the channel including the transmembrane segments, loops (Monks et al., 1999; Hong and Miller, 2000; Li-Smerin et al., 2000a, 2000b), and T1 (reported here) experience a conformational change during gating. A literal interpretation of these experiments would be that "the gate" is everywhere. A more structurally sensible interpretation is that the quaternary structure rearrangement that occurs as the channel moves between the open and closed states involves most of the channel complex. Residues in subunit interfaces or domain interfaces within the channel complex may be particularly good candidates for changes in state-dependent contacts.

### Replacement of T1 Suggests a Role for Stabilization of the Closed State

Replacement of T1 with a four-stranded coiled-coil restores efficient channel assembly but results in channels with an altered voltage-dependence that is identical to the T1-deletion mutant (Zerangue et al., 2000). Similar

results are shown here with Kv1.2. Kv1.2 does not assemble efficiently in the absence of T1 in our hands. Replacement of T1 with a four-stranded coiled-coil results in functional channels having a significant shift of $V_{1/2}$ in the hyperpolarizing direction (−30 mV) that is independent of the length and composition of the linker between the coils and the membrane-spanning part of the channel. These results lend further support to the idea that T1 contributes to the energetic stability of the closed state of the channel. T1 may also participate in the actual activation process, since these channels as well as functional *Shaker* channels missing T1, activate more slowly than their wild-type counterparts (Zerangue et al., 2000; Kobertz and Miller, 1999). The exact manner in which this occurs requires a more detailed study.

### Relevance of the T1 Structure to the Intact Channel

Recently, it has been suggested that the crystal structure of T1 does not accurately represent the conformation of T1 in the intact channel (Kobertz and Miller, 1999). While possible, the extreme stability of the T1 tetramer (~30 kcal mol$^{-1}$ at 1 M standard state) seems to make this proposal highly unlikely. The effective concentration of protein groups held in close proximity through intramolecular interactions can exceed tens of molar (Creighton, 1993). Although not known exactly, the effective concentration of the T1 domains in the context of the fully assembled channel is likely to be quite high. Given the amount of folding energy present in the T1 self-association, complete disruption of the T1 structure would require that the rest of the channel structure, in the fully assembled state, provide an equivalent, or greater amount of interaction energy to permanently disrupt the crystallographic structure into an alternative conformation. The findings that deletion of T1 destabilizes the closed state of the channel and that amino acid changes on complementary surfaces of T1 interface affect channel gating properties strongly suggest that the crystallographic structure, representing the lowest energy state of the T1 domain, corresponds to the T1 conformation in the closed state of the channel. Although the channel itself may not be able to provide sufficient energy to disrupt the T1 subunit interface, it seems possible that energy derived from conformational changes in the channel resulting from changes in the transmembrane potential could (estimated to be on the order of ~10 kcal mol$^{-1}$ for a $\Delta\Psi$ from −60 to 0 mV; see Sigworth, 1993).

The discovery that mutations in the polar core between subunits of Kv1.2 affect voltage-dependent channel activation suggests that changes in membrane potential elicit global conformational changes in the channel protein that include T1 as well as the transmembrane segments. The interfacial location of mutations that stabilize the closed channel and increase the global stability of the isolated T1 tetramers without altering its exterior appearance suggests that the tetrameric structure in the crystal represents the conformation of T1 when the channel is closed. Our studies provide a structural and conceptual platform for beginning to understand the physical basis for T1 function with respect to channel gating. Toward this end, it will be important to characterize where exactly T1 acts in the well-characterized activation pathway of Kv channels (Zagotta et al., 1994; Schoppa and Sigworth, 1998).

Kv1.2 activity can be modulated by phosphorylation (Huang et al., 1993, 1994; Lev et al., 1995; Tsai et al., 1999), or interaction with small GTPases (Cachero et al., 1998). These factors may operate in part through T1, altering its stability in the closed or open state. In this way, T1 may help connect the excitability properties of the channel to other cellular pathways in a reversible, regulated fashion.

## Experimental Procedures

### Protein Expression and Purification

Kv1.2 (McKinnon, 1989) residues 33–125 (CORE) and 33–138 (+13C) including a terminal stop codon were cloned into the NdeI and HinDIII sites of pET24B (Novagen) by PCR and verified by DNA sequencing. Proteins were expressed in *E. coli* BL21(DE3)pLysS induced at 0.4–0.8 $OD_{600}$ nm with 400 μM isopropyl-β-D-thiogalactoside (IPTG) for 3 hr. Cells were harvested and frozen. Cells were lysed by sonication in a buffer of 100 mM KCl, 50 mM NaCl, 10% glycerol, 20 mM n-octyl-β-D-glucopyranoside (OG) (SOL-GRADE, Anatrace), and 20 mM HEPES (pH 7.5). The insoluble fraction was removed by centrifugation for 30 min at 27,000 × g (Sorvall SS-34 rotor, 4°C). CORE was precipitated with 45% ammonium sulfate for 20 min on ice and recovered by centrifugation for 30 min at 27,000 × g (Sorvall SS-34 rotor, 4°C). The pellet was resuspended in 20 mM KCl, 1 mM EDTA, and 10 mM $NaC_2H_3O_2$ (pH 5.4) and purified by elution from a POROS/HS (Perseptive Biosystems) column using a linear gradient from 0.01–0.5 M KCl in this buffer. Fractions containing CORE were concentrated (Centriprep 10, Amicon) and exchanged into 100 mM KCl, 1 mM EDTA, and 20 mM phosphate (pH 7.2). Final purification was achieved with size exclusion chromatography (Superdex 200, Pharmacia) in 100 mM KCl, 1 mM EDTA, and 20 mM phosphate (pH 7.2). Protein was concentrated to ~10 mg ml$^{-1}$ (Centricon 10, Amicon). +13C proteins were purified in a similar fashion. Point mutants were made in double-stranded plasmids (Quickchange, Stratagene) and verified by complete DNA sequencing. +13C-T46D and VCORE formed inclusion bodies. Following cell lysis, the insoluble pellet was recovered and dissolved in a solution of 6M Gdm HCl, 100 mM KCl, 20 mM OG, 1 mM EDTA, and 20 mM HEPES (pH 7.5) and dialyzed in 3500 MWCO tubing against 100 mM KCl, 20 mM OG, 1 mM EDTA, and 20 mM HEPES (pH 7.5) for 12 hr at 4°C. T46D was insoluble in the absence of denaturant and was dialyzed into the same solution containing 1 M Gdm HCl. Insoluble material was removed by centrifugation for 30 min at 27,000 × g (Sorvall SS-34 rotor, 4°C). The soluble fraction containing refolded VCORE was purified by gel filtration as described above. +13C-T46D was purified by gel filtration in the presence of 1 M Gdm HCl.

### Protein Crystallization and Data Collection

Crystals were grown by vapor diffusion at 18°C. CORE at 5–10 mg ml$^{-1}$ crystallized in 9% PEG 1500, 5% n-propanol, 120 mM Gdm HCl, and 50 mM MES (pH 6.5) over the same solution with an extra 0%–15% water. +13C at 5–10 mg ml$^{-1}$ crystallized in 19% PEG 4000, 100 mM $NH_4$ $C_2H_3O_2$, 21% methanol, and 50 mM MES (pH 6.5). CORE crystals were soaked sequentially in 9.5% PEG 1500, 15% n-propanol, and 50 mM MES (pH 6.5) and 9.5% PEG 1500, 25% n-propanol, and 50 mM MES (pH 6.5) for ~15 min each prior to flash freezing in liquid nitrogen. +13C crystals were harvested directly into well solution and flash frozen. VCORE at 5–10 mg ml$^{-1}$ crystallized in 22% PEG 1500, 5% isopropanol, 200 mM $NaC_2H_3O_2$, 12 mM $SrCl_2$, and 50 mM Tris (pH 8.5) following streak-seeding (McPherson, 1999) from small VCORE crystals grown in similar solutions. VCORE crystals were soaked in 23% PEG 1500, 10% isopropanol, 200 mM $NaC_2H_3O_2$, 12 mM $SrCl_2$, and 50 mM Tris (pH 8.5) for ~15 min prior to flash freezing. Data for CORE were collected on a Rigaku-200 rotating anode (Raxis-IIc detector). Data for +13C and VCORE were collected at Beamline 5.0.2, Advanced Light Source,

Lawrence Berkeley Laboratory, (ADSC CCD detector). All data were processed with DENZO/SCALEPACK (Otwinowski and Minor, 1997), and ported into the CCP4 (Collaborative Computational Project, 1994). Molecular replacement using a polyserine model from the AKv1.1 T1 domain (Kreusch et al., 1998) was carried out with AMoRe (Navaza, 1994). In each case, a small set of unambiguous solutions was obtained that differed by 90° rotations from each other about the molecular 4-fold axis. Polyserine replacement models for CORE, +13C, and VCORE were rigid body refined with CNS (Brünger et al., 1998) (CORE) or REFMAC (Murshudov et al., 1997) (+13C and VCORE). Averaging and density modification were performed with native structure factors and polyserine model phases using DM (Cowtan, 1994) to produce unbiased maps for sidechain placement. Model building was done with O (Jones et al., 1991), and subsequent refinement employed CNS (Brünger et al., 1998) (CORE) or REFMAC/ARP (Murshudov et al., 1997) (+13C and VCORE).

### Electrophysiology

Kv1.2 (McKinnon, 1989) was cloned into a pGEMHE (Liman et al., 1992) derivative. Mutations were made in double-stranded plasmids (Quickchange, Stratagene) and confirmed by complete DNA sequencing. The p-IL sequence was obtained by PCR from a synthetic gene encoding the protein sequence: RMKQIEDKLEEILSKLYHIE NELARIKKLLGER. Kv1.2_LZ, and Kv1.2_LZ-linker comprised this sequence followed by a Gly-Ser-Gly spacer and Kv1.2 residues 134–499 or GGSGGS and Kv1.2 residues 160–499. RNA transcripts were made with the Ampliscribe kit (Epicenter Technologies) from DNA template linearized with NheI. Oocytes were surgically removed from anethestized frogs and treated with 2 mg $ml^{-1}$ collagenase (Worthington) in 96 mM NaCl, 2 mM KCl, 1 mM $MgCl_2$, and 5 mM HEPES (pH 7.5) at room temperature, ~1–2 hr. Two-electrode voltage clamp recordings were made on defolliculated stage V-VI *Xenopus laevis* oocytes microinjected with ~5–10 ng of RNA transcript. Initial recordings of the T46V mutant were made 72–144 hrs post-injection in a bath of 90Na solution (90 mM NaCl, 1 mM $MgCl_2$, and 10 mM HEPES [pH 7.5]). All other measurements were done in 90K solution (90 mM KCl, 1 mM $MgCl_2$, and 10 mM HEPES [pH 7.5]). Electrodes were pulled (pp-83, Narishige), filled with 3 M KCl, and had resistances of 0.1–1.5 MΩ. Recordings and voltage steps were controlled by a Pentium 66 computer (Dell) with CLAMPEX7 (Axon Instruments) and a Geneclamp500 Amplifier (Axon Instruments). Data were filtered at 2 kHz and leak subtracted with a P/8 protocol. Membrane potential was held at −80 (−70) mV and depolarized from −90 to 65 (60) mV in 5 (10) mV steps followed by a tail current command of −80 (−60) mV (parenthesis designate 90Na solution protocol). I-V curves were generated from tail-current measurements taken at a fixed time point following the tail current command step. Data were normalized to the maximal values obtained in each individual oocyte (I/Imax) and were with a first-order Boltzmann function to obtain $V_{1/2}$. In all cases, $\Delta V_{1/2}$ values were obtained by comparison to wild-type Kv1.2 in the same oocyte batch.

### Protein Stability Measurements

Protein concentrations were determined by absorbance (Edelhoch, 1967). Denaturation was measured by circular dichroism at 220 nm as a function of GdmHCl. Stock solutions containing 100 mM KCl, 10 mM phosphate, and 0–6 M GdmHCl (0.5 M increments) were prepared using Ultrapure GdmHCl (ICN #105696) and adjusted directly to pH 7.2. Intermediate concentrations were prepared by stock solution mixing. Protein samples (10 μM monomer) were equilibrated at room temperature for at least 48 hr. Equilibrium was reached within 40 hr (determined from measurements in which the protein was transferred to the middle of the folding transition following incubation under folded or denatured conditions). No changes were seen in the unfolding curve up to one month following the preparation of the samples. Circular dichroism measurements were made at 20°C with a JASCO J-710 spectropolarimeter equipped with a peltier temperature control. Spectra were collected from 195–320 nm in 1 nm steps in a 0.2 cm quartz cuvette as an average of five scans. The ΔG of unfolding was calculated at 1 M standard state using a monomer to tetramer equilibrium as described (Pace et al., 1989). Relative differences in the free energy changes were expressed as $\Delta\Delta G_f = \Delta G_{mutant(0\ M\ GdmHCl)} - \Delta G_{wild\ type(0\ M\ GdmHCl)}$.

### Acknowledgments

We thank T. Earnest and staff at ALS beamline 5.0.2 for help with data collection; S. Jaswal and D. A. Agard for use of the CD; M. Yu for molecular biology assistance; and members of the Jan lab for helpful discussions. D. L. M. thanks R. Aldrich, D. Barrick, E. Isacoff, and N. Unwin for insightful discussions. Y. N. Jan and L. Y. Jan are HHMI investigators. This work was supported by an NIH grant.

Received December 15, 1999; revised June 23, 2000.

### References

Armstrong, C.M., and Hille, B. (1972). The inner quaternary ammonium ion receptor in potassium channels of the node of Ranvier. J. Gen. Physiol. *59,* 388–400.

Ascher, P., and Stevens, C. (1992). Signaling mechanisms. Curr. Opin. Neurobiol. *2,* 241–242.

Bixby, K.A., Nanao, M.H., Shen, N.V., Kreusch, A., Bellamy, H., Pfaffinger, P.J., and Choe, S. (1999). $Zn^{2+}$-binding and molecular determinants of tetramerization in voltage-gated $K^+$ channels. Nature Struct. Biol. *6,* 38–43.

Brünger, A.T., Adams, P.D., Clore, G.M., DeLano, W.L., Gros, P., Grosse-Kunstleve, R.W., Jiang, J.-S., Kuszeski, J., Nilges, M., Pannu, N.S., et al. (1998). Crystallography and NMR system: a new software suite for macromolecular structure determination. Acta Crystallogr. D *54,* 905–921.

Cabral, J.H., Lee, A., Cohen, S.L., Chait, B.T., Li, M., and MacKinnon, R. (1998). Crystal structure and functional analysis of the HERG potassium channel N termius: a eukaryotic PAS domain. Cell *95,* 649–655.

Cachero, T.G., Morielli, A.D., and Peralta, E.G. (1998). The small GTP-binding protein RhoA regulates a delayed rectifier potassium channel. Cell *93,* 1077–1085.

Carson, M. (1991). Ribbons 2.0. J. Appl. Cryst. *24,* 958–961.

Cha, A., and Bezanilla, F. (1997). Characterizing voltage-dependent conformational changes in the *Shaker* $K^+$ channel with flourescence. Neuron *19,* 1127–1140.

Chandy, K.G., and Gutman, G.A. (1995). Voltage-gated potassium channel proteins. In Handbook of Receptors and Channels, R.A. North, ed. (Boca Raton: CRC Press), pp. 1–71.

Chiara, M.D., Monje, F., Castellano, A., and López-Barneo, J. (1999). A small domain in the N terminus of the regulatory α-subunit Kv2.3 modulates Kv2.1 potassium channel gating. J. Neurosci. *19,* 6865–6873.

Clackson, T., and Wells, J.A. (1995). A hot spot of binding energy in a hormone-receptor interface. Science *267,* 383–386.

Collaborative Computational Project N. (1994). The CCP4 suite: programs for protein crystallography. Acta Crystallogr. A *50*, 760–763.

Cowtan, K. (1994). DM: An automated procedure for phase improvement by density modification. Joint CCP4 and ESF-EACMB Newsletter on Protein Crystallography *31*, 34–38.

Creighton, T.E. (1993). Proteins: Structures and Molecular Properties, Second Edition (New York: W.H. Freeman).

Cunningham, B.C., and Wells, J.A. (1989). High-resolution epitope mapping of hGH-receptor interactions by alanine-scanning mutagenesis. Science *244,* 1081–1085.

Cushman, S.J., Nanao, M.H., Jahng, A.W., DeRubies, D., Choe, S., and Pfaffinger, P.J. (2000). Voltage dependent activation of potassium channels is coupled to T1 domain structure. Nat. Struct. Biol. *7,* 403–407.

del Camino, D., Holmgren, M., and Yellen, G. (2000). Blocker protection in the pore of a voltage-gated $K^+$ channel and its structural implications. Nature *403,* 321–325.

Doyle, D.A., Cabral, J.M., Pfuetzner, R.A., Kuo, A., Gulbis, J.M., Cohen, S.L., Chait, B.T., and Mackinnon, R. (1998). The structure of the potassium channel: molecular basis of $K^+$ conduction and selectivity. Science *280,* 69–77.

Edelhoch, H. (1967). Spectroscopic determination of tryptophan and tyrosine in proteins. Biochemistry *6,* 1948–1954.

Elkes, D.A., Cardozo, D.L., Madison, J., and Kaplan, J.M. (1997). EGL-36 *Shaw* channels regulate *C. elegans* egg-laying muscle activity. Neuron *19,* 165–174.

Harbury, P.B., Zhang, T., Kim, P.S., and Alber, T. (1993). A switch between two-, three-, and four-stranded coiled coils in GCN4 leucine zipper mutants. Science *262,* 1401–1407.

Heginbotham, L., Lu, Z., Abramson, T., and MacKinnon, R. (1992). Mutations in the $K^+$ channel signature sequence. Biophys. J. *66,* 1061–1067.

Hendsch, Z., and Tidor, B. (1999). Electrostatic interactions in the GCN4 leucine zipper: substantial contributions arise from intramolecular interactions enhanced on binding. Prot. Sci. *8,* 1381–1392.

Hendsch, Z.S., and Tidor, B. (1994). Do salt bridges stabilize proteins? A continuum electrostatic analysis. Prot. Sci. *3,* 211–226.

Hille, B. (1992). Ionic Channels of Excitable Membranes (Sunderland, MA: Sinauer Associates, Inc.).

Hirsch, J.A., Schubert, C., Gurevich, V.V., and Sigler, P.B. (1999). The 2.8 Å crystal structure of visual arrestin: a model for arrestin's regulation. Cell *97,* 257–269.

Holmgren, M., Smith, P.L., and Yellen, G. (1997). Trapping of organic blockers by closing of voltage-dependent $K^+$ channels: evidence for a trap door mechanism in activation gating. J. Gen. Physiol. *109,* 527–535.

Hong, K.H., and Miller, C. (2000). The lipid-protein interface of a *Shaker* $K^+$ channel. J. Gen. Physiol. *115,* 51–58.

Huang, X.-Y., Morielli, A.D., and Peralta, E.G. (1993). Tyrosine kinase-dependent suppression of a potassium channel by the G protein-coupled m1 muscarinic acetylcholine receptor. Cell *75,* 1145–1156.

Huang, X.-Y., Morielli, A.D., and Peralta, E.G. (1994). Molecular basis of cardiac potassium channel stimulation by protein kinase A. Proc. Natl. Acad. Sci. USA *91,* 624–628.

Isacoff, E.Y., Jan, Y.N., and Jan, L.Y. (1991). Putative receptor for the cytoplasmic inactivation gate in the *Shaker* $K^+$ channel. Nature *353,* 86–90.

Jan, L.Y., and Jan, Y.N. (1997). Cloned potassium channels from eukaryotes and prokaryotes. Annu. Rev. Neurosci. *20,* 91–123.

Janin, J., Miller, S., and Chothia, C. (1988). Surface, subunit interfaces and interior of oligomeric proteins. J. Mol. Biol., 155–164.

Javadpour, M.M., Eilers, M., Groesbeek, M., and Smith, S.O. (1999). Helix packing in polytopic membrane proteins: Role of glycine in transmembrane helix association. Biophys. J. *77,* 1609–1618.

Johnstone, D.B., Wei, A., Butler, A., Salkoff, L., and Thomas, J.H. (1997). Behavioral defects in *C. elegans egl-36* mutants result from potassium channels shifted in voltage-dependence of activation. Neuron *19,* 151–164.

Jones, S., and Thornton, J.M. (1997). Analysis of protein-protein interaction sites using surface patches. J. Mol. Biol. *272,* 121–132.

Jones, T.A., Zou, J.Y., Cowan, S.W., and Kjeldgaard, M. (1991). Improved methods for building protein models in electron density maps and the location of errors in these models. Acta Crystallogr. A *47,* 110–119.

Kobertz, W.R., and Miller, C. (1999). $K^+$ channels lacking the 'tetramerization' domain: implications for pore structure. Nature Struct. Biol. *6,* 1122–1125.

Kreusch, A., Pfaffinger, P.J., Stevens, C.F., and Choe, S. (1998). Crystal structure of the tetramerization domain of the *Shaker* potassium channel. Nature *392,* 945–948.

Lev, S., Moreno, H., Martinez, R., Canoll, P., Peles, E., Musacchio, J.M., Plowman, G.D., Rudy, B., and Schlessinger, J. (1995). Protein tyrosine kinase PYK2 involved in $Ca^{2+}$-induced regulation of ion channel and MAP kinase functions. Nature *376,* 737–745.

Li, M., Jan, Y.N., and Jan, L.Y. (1992). Specification of subunit assembly by the hydrophillic amino-terminal domain of the *Shaker* potassium channel. Science *257,* 1225–1230.

Li-Smerin, Y., Hackos, D., and Swartz, K. (2000a). $\alpha$-helical structural elements within the voltage-sensing domains of a $K^+$ channel. J. Gen. Physiol. *115,* 33–49.

Li-Smerin, Y., Hackos, D.H., and Swartz, K.J. (2000b). A localized interaction surface for voltage-sensing domains on the pore domain of a $K^+$ channel. Neuron *25,* 411–423.

Liman, E.R., Tytgat, J., and Hess, P. (1992). Subunit stoichiometry of a mammalian $K^+$ channel determined by construction of multimeric cDNAs. Neuron *9,* 861–871.

Liu, Y., Holmgren, M., Jurman, M.E., and Yellen, G. (1997). Gated access to the pore of a voltage-dependent $K^+$ channel. Neuron *19,* 175–184.

Lopez, G.A., Jan, Y.N., and Jan, L.Y. (1994). Evidence that the S6 segment of the *Shaker* voltage-gated $K^+$ channel comprises part of the pore. Nature *367,* 179–182.

Mannuzzu, L.M., Morone, M.M., and Isacoff, E.Y. (1996). Direct physical measure of conformational rearrangement underlying potassium channel gating. Science *271,* 213–216.

McKinnon, D. (1989). Isolation of a cDNA clone coding for a putative second potassium channel indicates the existence of a gene family. J. Biol. Chem. *264,* 8230–8236.

McPherson, A. (1999). Crystallization of Biological Macromolecules (Cold Spring Harbor, New York: Cold Spring Harbor Laboratory Press).

Monks, S.A., Needleman, D.J., and Miller, C. (1999). Helical structure and packing orientation of the S2 segment in the *Shaker* $K^+$ channel. J. Gen. Physiol. *113,* 415–423.

Murshudov, G.N., Vagin, A.A., and Dodson, E.J. (1997). Refinement of macromolecular structures by the maximum-likelihood method. Acta Crystallogr. D *53,* 240–255.

Navaza, J. (1994). AMoRe: an automated package for molecular replacement. Acta Crystallogr. A *50,* 157–163.

Nichols, A., Sharp, K., and Honig, B. (1991). Protein folding and association: insights from the interfacial and thermodynamic properties of hydrocarbons. Proteins. Struct. Func. Genet. *11,* 281–296.

Otwinowski, Z., and Minor, W. (1997). Processing of X-ray diffraction data collected in oscillation mode. Methods Enzymol. *276,* 307–326.

Pace, C.N., Shirley, B.A., and Thomson, J.A. (1989). Measuring the conformational stability of a protein. In Protein Structure: A Practical Approach, T.E. Creighton, ed. (Oxford: IRL Press), pp. 311–330.

Pons, J., Rajpal, A., and Kirsch, J.F. (1999). Energetic analysis of an antigen/antibody interface: alanine scanning mutagenesis and double mutant cycles on the HyHEL-10/lysozyme interaction. Prot. Sci. *8,* 958–968.

Schoppa, N.E., and Sigworth, F.J. (1998). Activation of *Shaker* potassium channels .III. an activation gating model for wild-type and V2 mutant channels. J. Gen. Physiol. *111,* 313–342.

Schulteis, C.T., Nagaya, N., and Papazian, D.M. (1996). Intersubunit interaction between amino- and carboxyl-terminal cysteine residues in tetrameric *Shaker* $K^+$ channels. Biochemistry *35,* 12133–12140.

Shen, N.V., Chen, X., Boyer, M.M., and Pfaffinger, P.J. (1993). Deletion analysis of $K^+$ channel assembly. Neuron *11,* 67–76.

Sigworth, F.J. (1993). Voltage gating of ion channels. Quart. Rev. Biophys. *27,* 1–40.

Tsai, W., Morielli, A.D., Cachero, T.G., and Peralta, E.G. (1999). Receptor protein tyrosine phophatase $\alpha$ participates in the m1 muscarinic acetylcholine receptor-dependent regulation of Kv1.2 channel activity. EMBO J. *18,* 109–118.

von Heijne, G. (1991). Proline kinks in transmembrane $\alpha$-helices. J. Mol. Biol. *218,* 499–503.

Waldberger, C.D., Schildbach, J.F., and Sauer, R.T. (1995). Are buried salt bridges important for protein stability and conformational specificity? Nature Struct. Biol. *2,* 122–128.

Wells, J.A. (1991). Systematic mutation analyses of protein-protein interfaces. Methods Enzymol. *202,* 390–411.

Wimley, W.C., Gawrisch, K., Creamer, T.P., and White, S.H. (1996). Direct measurement of salt bridge solvation energies using a peptide model system: Implications for protein stability. Proc. Natl. Acad. Sci. USA *93,* 2985–2990.

Yellen, G. (1998). The moving parts of voltage-gated ion channels. Quart. Rev. Biophys. *31,* 239–295.

Zagotta, W.N., Hoshi, T., and Aldrich, R.W. (1994). *Shaker* potassium channel gating .III. evaluation of kinetic models for activation. J. Gen. Physiol. *103,* 321–362.

Zerangue, N., Jan, Y.N., and Jan, L.Y. (2000). An artificial tetramerization domain restores efficient assembly of functional Shaker channels lacking T1. Proc. Natl. Acad. Sci. USA *97,* 3591–3595.

**Protein Data Bank Accession Numbers**

Crystallographic coordinates for CORE, +13C, and VCORE have RCSB Protein Data Bank accession numbers 1QDW, 1QDV, and 1DSX, respectively.